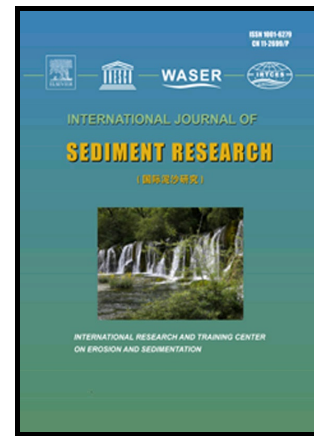


Author's Accepted Manuscript

Morphological reactions of schematic alluvial rivers: long simulations with a 0-D model

M. Franzoia, M. Nones



www.elsevier.com/locate/ijsrc

PII: S1001-6279(17)30116-6
DOI: <http://dx.doi.org/10.1016/j.ijsrc.2017.04.002>
Reference: IJSRC112

To appear in: *International Journal of Sediment Research*

Received date: 20 April 2016
Revised date: 10 March 2017
Accepted date: 14 April 2017

Cite this article as: M. Franzoia and M. Nones, Morphological reactions of schematic alluvial rivers: long simulations with a 0-D model, *International Journal of Sediment Research*, <http://dx.doi.org/10.1016/j.ijsrc.2017.04.002>

This is a PDF file of an unedited manuscript that has been accepted for publication. As a service to our customers we are providing this early version of the manuscript. The manuscript will undergo copyediting, typesetting, and a review of the resulting galley proof before it is published in its final citable form. Please note that during the production process errors may be discovered which could affect the content, and all legal disclaimers that apply to the journal pertain.

Morphological reactions of schematic alluvial rivers: long simulations with a 0-D model

M. Franzoia^a, M. Nones^{b,*}

^aPhD, Department of Civil, Environmental and Architectural Engineering, University of Padova, via Marzolo 9, 35131 Padova, Italy

^bPhD, Interdepartmental Centre for Industrial Research in Building and Construction - Fluid Dynamics Unit, University of Bologna Via del Lazzaretto 15/5, 40131 Bologna, Italy

michael.nones@unibo.it

Abstract

The paper presents a 0-D model of an alluvial watercourse schematized in two connected reaches, evolving at the long time-scale and under the hypothesis of Local Uniform Flow. Each reach is defined by its geometry (constant length and width, time-changing slope) and grain-size composition of the bed, while the sediment transport is computed using a sediment rating curve. The slope evolution is provided by a 0-D mass balance and the evolution of the bed composition is computed by a 0-D Hirano equation. A system of differential equations, solved with a predictor-corrector scheme, is derived and applied to the schematic watercourse to simulate the morphological response to changing initial conditions, and the evolution towards long-term equilibrium conditions. Differently from a single-reach 0-D schematization with uniform grain-size, besides the simplifications adopted, the model proposed here simulates the behaviour of alluvial rivers in a physically-based way, showing a grain-size fining in the downstream direction accompanied by milder slopes, and a tendency to develop concave longitudinal profiles.

Keywords

Alluvial rivers, Local Uniform Flow, Morphological equilibrium, Physically-based 0-D model, River morphology, Sediment transport

Notation

B	mean river width (m)
c_1	integration constant (-)
c_2	integration constant (-)
d	ratio between d_f and d_c (-)
d_c	diameter of the coarse fraction of sediments (m)
d_f	diameter of the fine fraction of sediments (m)
d_{eq}	equivalent diameter of sediments (m)
d_k	size of the k -th fraction of sediments (m)
Fr	Froude number (-)
g	dimensionless sediment transport at the input point (-)
G	sediment transport at the input point ($\text{m}^3 \text{s}^{-1}$)
h_i	dimensionless bottom level of the i -th reach (-)
H_i	bottom elevation of the i -th reach (m) $i = \text{index of the } i\text{-th reach: } i=U \text{ for the upstream reach, } i=D \text{ for the downstream one}$
i_i	dimensionless bottom slope of the i -th reach (-)
In	interface value (-)
I_i	bottom slope of the i -th reach (m/m)
k	index of the k -th fraction of sediments: $k=c$ for coarse sediments, $k=f$ for fine sediments
l_i	dimensionless length of the i -th reach (-)
L_i	length of the i -th reach (m)
m	exponent of the Engelund-Hansen formula (-)
m_{orph}	dimensionless morphodynamic parameter (-)
M	morphodynamic parameter ($(\text{m}^3 \text{s}^{-1})^{1-m}$)

n	exponent of the Engelund-Hansen formula (-)
p	exponent of the Engelund-Hansen formula (-)
p_i	dimensionless total sediment transport along the i -th reach (-)
P	total sediment transport (m^3s^{-1})
P_c	sediment transport of the coarse fraction of sediments (m^3s^{-1})
P_f	total sediment transport of the fine fraction of sediments (m^3s^{-1})
$P_{i,k}$	transport of the k -th fraction of the sediment along the i -th reach (m^3s^{-1})
q	exponent of the Engelund-Hansen formula (-)
Q	flow discharge (m^3s^{-1})
r	index of the r -th component: $r=0$ for the entire slope, $r=mix$ for the active layer
s	exponent of the Engelund-Hansen formula (-)
t	time (s)
t_0	initial time (s)
t_∞	equilibrium time (s)
$T_{r,i}$	filling time of the r -th component along the i -th reach (s)
T_w	forcing period (s)
$V_{r,i}$	filling volume of the r -th component along the i -th reach (m^3)
x	space (m)
Y	mean water depth (m)
α	composition of the total sediment transport along the i -th reach (-)
α_{EH}	proportional coefficient of the Engelund-Hansen formula (-)
α_G	composition of the sediment transport at the input point (-)
β	bottom composition (-)
β_i	bottom composition along the i -th reach (-)
β_l	vertical exchange of sediment between active layer and substrate (-)

- β_l^I vertical exchange of sediment between active layer and substrate (-) β_k^* = percentage of the k -th fraction of the sediments in the active layer (-)
- δ thickness of the active layer (m)
- ω angular frequency (-)
- χ Chézy roughness coefficient ($\text{m}^{1/2}\text{s}^{-1}$)
- ζ_k hiding-exposure coefficient (-)

1. Introduction

During the last decades, the availability of hydro-morphological and sedimentological models, combined with their accuracy, have increased enormously, giving reason to the development of new methodologies, models and approaches in the field of hydroinformatics and hydraulic modelling (Bai & Wang, 2014; Gourbesville, 2009; Hobley et al., 2017; Vidal et al., 2005). These new tools have contributed to improve the knowledge on the theoretical background and physical processes involved in modelling the Earth's landscape evolution, validating the assumptions made by modellers. As observed by various authors (e.g., Gourbesville, 2009; Guinot & Gourbesville, 2003; Hobley et al., 2017), physically-based models are often quite similar, having the schematization of the involved processes and the geometry of the domain as predominant factors. Therefore, a reliable and realistic schematization of alluvial rivers results fundamental for evaluating, among other things, the meaning and implications of the simplifications adopted, together with the effects of different initial and boundary conditions on the equilibrium river morphology.

In the present work, the term “equilibrium” defines a stationary morphological condition of the river system, related to specific space- and time-scales of the involved processes. Alluvial rivers are generally characterized by a profile that attains the equilibrium with respect to several forcing terms at the basin scale, where interactions between the watercourse and the local environment occur. For this analysis, the variables that describe the river behaviour are averaged over an appropriate time-scale, short enough to disregard the subsidence or the tectonic uplift effects, but long enough to neglect micro- (e.g. ripples and particles) and meso-forms (e.g. dunes) variations.

Besides other drivers, alluvial rivers are generally influenced by a quasi-steady annual fluctuation of initial and boundary conditions therefore, at the reach scale, their morphological characteristics (longitudinal and planimetric profiles, grain-size composition of the bed) remain quite stable over typical human observation time (decades or centuries). Indeed, this configuration can be defined “equilibrium state” and a sediment rating curve called “equilibrium curve” can be calibrated (e.g., Asselman, 2000; Colby, 1956; Franzoia, 2014; Horowitz, 2003; Walling, 1974). This curve, usually a power relationship, relates sediments and water fluxes by means of a proportionality coefficient, and can be useful in many cases, such as for hydropower reservoir management or dredging operations.

In recent years, many studies about the long-term morphological response of rivers to different hydrological constraints were performed. As an example, Tealdi et al. (2011) have found an analytical solution to evaluate the morphological variations of rivers affected by stepwise perturbations on both liquid and solid inputs (e.g., dam construction, river diversion). Considering a river with uniform grain-size and a variable width, these authors noticed that the variations of the mean river width were very small. Other authors schematized alluvial watercourses as unique zero-dimensional reaches with uniform sediment composition, postulating a time-dependent slope, but constant width and a single grain-size composition (Di Silvio & Nones, 2014).

In the present paper, it is assumed that a schematic river maintains its width within the same order of magnitude along the course. In this manner, the relative importance of the river width in the sediment transport formula can be supposed negligible with respect to that of slope and bed composition (namely, the width can be considered constant at the analysed scale). Adopting a 0-D model with liquid and solid inputs entering at the watershed barycenter, one can assume a constant width and a time-dependent bottom composition, limiting the errors with respect to real watercourses. The barycenter represents the upstream end of the river channel, where water and sediment inputs from the basin slopes are concentrated. The non-uniform and time-dependent grain-size composition of sediments plays an important role in the erosion and deposition processes, mainly at the small spatial scales, governing the armouring, but also at the large scale, influencing the planimetric stability of the river bed. The grain-size patchiness, in fact, is fundamental in the downstream fining process and in the evolution of the longitudinal profile, typically concave (e.g., Church & Ferguson, 2015; Costigan et al., 2014; Cui et al., 1996; Frings, 2008; Gasparini et al., 2004; Paola & Seal, 1995; Sinha & Parker, 1996). Integrating in space the

1-D hydro-morphodynamic system with the above-mentioned conditions, an implicit and non-linear system is obtained, which is not analytically solvable (Franzoia, 2014). Solving it numerically results extremely simpler and faster than applying a complete 1-D model based on similar hypotheses (Nones, 2012).

After a discussion of the approach adopted, the model is applied to a simplified watercourse for studying the long-term behaviour of concave-profiled rivers, namely answering to the following questions:

- How and in how much time a schematic river can reach the equilibrium state?
- If it is already in equilibrium, how does the river react to an impulse or a periodic variation of its initial conditions?
- Can the two-reach model with variable grain-size composition represents the behaviour of alluvial rivers in a more realistic and physically-based way, with respect to the single-reach model with uniform grain-size proposed by Di Silvio and Nones (2014)?

The paper is structured as follow. After a theoretical development of the 0-D model, highlighting the principal hypotheses and simplifications adopted, the reactions of a schematic river to different perturbations of the initial conditions are analysed. In detail, these perturbations regard the sediment input amount (stepwise and sinusoidal variations) and the input of the water discharge. To demonstrate the capability of the model to represent different temporal scales, an analysis of the very long-term evolution is also reported. Final conclusions highlight strengths and weaknesses of the adopted approach, and present open questions for scholars and researchers in modelling the long-term evolution of alluvial watercourses.

2. Methods

2.1 Development of the 0-D model

The 1-D hydro-morphodynamic model is integrated along a schematic alluvial river under two hypotheses: instantaneous water flow propagation and Local Uniform Flow (LUF) conditions (Fasolato et al., 2009, 2011; Nones & Di Silvio, 2016). This latter hypothesis, which assumes that the averaged energy line and the averaged water and bottom profiles have the same slope, links the description of the hydro-morphodynamics to the Froude number of the studied reach (Nones, 2012). To describe the solid phase, only a bimodal mixture has been considered here, assuming two representative grain-size classes ($k=2$) that characterize fine and coarse fractions of the

sediments. Furthermore, no changes due to climate or anthropogenic actions alter the river evolution, but the initial conditions.

To develop a 0-D model representing the concave longitudinal profile typical of alluvial rivers, the stream is schematized with two linked LUF reaches, having constant width and length. The upstream reach, indicated with the subscript U , goes from the barycenter of the watershed to the conjunction point, while the downstream one (subscript D), goes from the conjunction point to the outlet (Fig. 1). In the figure, L and H indicate the reach length and elevation, respectively, with the latter evolving from the initial status at the time t_0 towards the equilibrium H_∞ at the time t_∞ . G represents the input of sediment transport from the upstream end of the system, while P is the sediment flow that comes out from the watercourse. Under a physical point of view, the two reaches can represent the highland and the lowland part of alluvial rivers, characterized by higher slopes and coarser sediments and milder slope and finer sediments, respectively.

For each reach, the typical load duration curve is assumed constant, accounting for the equations typically applied in simplified 1-D hydro-morphodynamic models (Fasolato et al., 2009). Considering well-developed sub-critical ($Fr < 0.8$) or super-critical ($Fr > 1.2$) Froude regions, such models decouple the hydrodynamics and the morphodynamics (De Vriend et al., 1993; Juez et al., 2013), when considering both sediment (Lyn, 1987; Lyn & Altinakar, 2002) and graded sediment (Stecca et al., 2014). Therefore, it is possible to adopt the 1-D sediment continuity (eq. 1) developed by Exner (1920), and the mass balance for each grain-size fraction of the active layer (2), computed following Hirano (1971).

In the present approach, the Eulerian framework is adopted, averaging the quantities involved over a finite spatial and temporal scale (Ballio et al., 2014).

$$B \frac{\partial H}{\partial t} = - \sum_{k=1}^2 \frac{\partial P_k}{\partial x} \quad (1)$$

$$\delta B \frac{\partial [\beta_1(x)]}{\partial t} = - \frac{\partial P_k}{\partial x} - \beta_1^{In}(x) B \frac{\partial H}{\partial t} \quad (2)$$

where B is the river width, here assumed as constant, P_k indicates the transport of the k -th fraction of the sediments, H represents the bed elevation above a reference level. Assuming a single active layer having a thickness δ , β_1 represents the vertically-averaged grain-size distribution within the active layer, while β_1^{In} is the vertical exchange of sediment between active layer and substrate, indicating the interface value with the subscript In .

Eqs. (1) and (2) are integrated along the longitudinal axis x : from $x=0$, where the inputs of liquid and solid discharges are concentrated, to $x=L_U$ for the upstream reach and from $x=L_U$ to $x=L_U+L_D$ for the downstream one (Fig. 1):

$$\left\{ \begin{array}{l} \int_0^{L_U} B \frac{\partial H_U}{\partial t} dx + \int_0^{L_U} B \frac{\partial P_U}{\partial x} dx = 0 \\ \int_0^{L_U} \delta B \frac{\partial \beta_{U,k}(x)}{\partial t} dx + \int_0^{L_U} \frac{\partial P_{U,k}}{\partial x} dx + \int_0^{L_U} B \beta_{U,k}(x) \frac{\partial H_U}{\partial t} dx = 0 \\ \int_{L_U}^{L_U+L_D} B \frac{\partial H_D}{\partial t} dx + \int_{L_U}^{L_U+L_D} B \frac{\partial P_D}{\partial x} dx = 0 \\ \int_{L_U}^{L_U+L_D} \delta B \frac{\partial \beta_{D,k}(x)}{\partial t} dx + \int_{L_U}^{L_U+L_D} \frac{\partial P_{D,k}}{\partial x} dx + \int_{L_U}^{L_U+L_D} B \beta_{D,k}(x) \frac{\partial H_D}{\partial t} dx = 0 \end{array} \right. \quad (3)$$

In the conjunction point $x=L_U$ the continuity requires that the upstream transport of each fraction equals the downstream one $P_{U,k}(x=L_U)=P_{D,k}(x=L_U)$, which means that the respective percentages are equal $\beta_{U,k}(x=L_U)=\beta_{D,k}(x=L_U)$.

Applying the divergence theorem one obtains:

$$\left\{ \begin{array}{l} \overline{BL_U} \frac{d\overline{H_U}}{dt} + [P_U(x=L_U, t)] - [P_U(x=0, t)] = 0 \\ L_U \overline{\delta B} \frac{d\overline{\beta_{U,k}}}{dt} + [P_{U,k}(x=L_U, t)] - [P_{U,k}(x=0, t)] + \overline{BL_U} \overline{\beta_{U,k}} \frac{d\overline{H_U}}{dt} = 0 \\ \overline{BL_D} \frac{d\overline{H_D}}{dt} + [P_D(x=L_U+L_D, t)] - [P_U(x=L_U, t)] = 0 \\ L_D \overline{\delta B} \frac{d\overline{\beta_{D,k}}}{dt} + [P_{D,k}(x=L_U+L_D, t)] - [P_{D,k}(x=L_U, t)] + \overline{BL_D} \overline{\beta_{D,k}} \frac{d\overline{H_D}}{dt} = 0 \end{array} \right. \quad (4)$$

where the values spatially averaged over the reach are represented by an overline.

The 0-D model is defined by two connected LUF reaches, each one characterized by a uniform slope equal to the mean slope $\overline{I_U}(t)$ and $\overline{I_D}(t)$, for the upstream and the downstream reach, respectively. These two slopes are univocally related to the mean relief elevations $\overline{H_U}(t)$ and $\overline{H_D}(t)$, and can be respectively computed as $\overline{I_U}(t)=\overline{H_U}(t)/\overline{L_U}=2\overline{H_U}(t)/L_U$ having $\overline{L_U}=L_U/2$; and $\overline{I_D}(t)=\overline{H_D}(t)/\overline{L_D}=2\overline{H_D}(t)/L_D$ with $\overline{L_D}=L_D/2$.

2.2 Solid transport expressions

Through a sediment transport formula of the Engelund-Hansen type (1967) to express the relationship between liquid and solid flows (e.g., Armanini & Di Silvio, 1988), the sediment transport P_k for each sediment fraction k passing through a section can be computed as:

$$P_k(x, t) = \alpha_{EH} \frac{Q(x, t)^m}{B(x, t)^p} \frac{I(x, t)^n}{d_k^q} \beta_k(x, t) \zeta_k(x, t) \quad (5)$$

where α_{EH} is a proportionality coefficient, I represents the local bottom slope (coincident with energy line and water profile slopes under the LUF hypothesis), d_k is the diameter of the k -th fraction of sediments and ζ_k is the hiding-exposure coefficient, which considers the effect of the mutual influence of grains of different sizes (Ribberink, 1987).

$$\zeta_k(x, t) = \left[d_k / \sum_{k=1}^2 \beta_k(x, t) d_k \right]^s \quad (6)$$

Regarding eq. 5, the exponent m , which generally spans between 1.5 and 2.5, is a site-specific parameter that should be calibrated for each river, depending on what uniform flow equation is adopted (Basile, 1994; Nones, 2012), and the exponents n , p and q are proportional to it. Adopting the Chézy formula $Q = \chi B Y^{3/2} I^{1/2}$, where χ represents the Chézy roughness and Y is the mean water depth, one obtains $n=m$, $p=(m-1)$ and $q=3/2(m-1)$. The exponent s (eq. 6) ranges between 0 and 1, depending on the bed composition: the finer is the characteristic diameter, the smaller the exponent s is.

For the sake of simplicity, only two representative grain-size classes are considered in the present approach: coarse and fine fractions are indicated with the subscript c and f , respectively. Starting from the previous equations and neglecting the subscript k , one can assume that β represents the bottom composition of the fine sediment characterized by a diameter d_f and, therefore, $1-\beta$ is the composition of the coarse material having a diameter d_c .

The total sediment transport of the fine fraction is given by:

$$P(x, t) = \alpha_{EH} \frac{Q(x, t)^m}{B(x, t)^p} \frac{I(x, t)^n}{d_{eq}(x, t)^q} \quad (7)$$

where d_{eq} represents the equivalent diameter of the bottom (Nones, 2012)

$$d_{eq}(x, t)^q = \frac{\beta(x, t) \left[(1/d)^{q-s} - 1 \right] + 1}{d_c^q \left[\beta(x, t)(d-1) + 1 \right]^s} \quad (8)$$

where $d=d_f/d_c$ is the ratio between fine and coarse fractions.

The composition of the total sediment transport $\alpha=P_f(t)/P(t)$ (or $1-\alpha=P_c(t)/P(t)$) depends on the bottom composition of the fine sediment β .

$$\alpha(x,t) = \frac{\beta(x,t)(1/d)^{q-s}}{\beta(x,t)\left[(1/d)^{q-s} - 1\right] + 1} \quad (9)$$

Representing all the coefficients and the morphological parameters in a unique parameter M called “morphodynamic parameter”, one obtains a sediment rating curve (Asselman, 2000; Horowitz, 2003).

In the present model, the river width B is time-averaged and assumed constant, because its influence on the sediment transport results negligible with respect to the other parameters (Franzoia, 2014).

$$P(t) = \alpha_{EH} \frac{1}{B^p} \frac{\bar{I}(t)^n}{d_{eq}(t)^q} Q(t)^m = M(t)Q(t)^m \quad (10)$$

The morphodynamic parameter $M(t)$ is time-dependent, namely a function of the time-variable parameters $\bar{I}(t)$ and $\bar{\beta}(t)$.

$$M(t) = \alpha_{EH} \frac{\bar{I}(t)^n}{B^p} \frac{\bar{\beta}(t)\left[(1/d)^{q-s} - 1\right] + 1}{d_c^q \left[\bar{\beta}(t)(d-1) + 1\right]^s} = \alpha_{EH} \frac{\bar{I}(t)^n}{B^p} c_1 \left[\bar{\beta}(t)\right] = Cost \cdot \bar{I}(t)^n c_1 \left[\bar{\beta}(t)\right] \quad (11)$$

where $Cost$ sums up all the constant parameters and c_1 is an implicit function of $\bar{\beta}(t)$ and d .

$$c_1 \left[\bar{\beta}(t)\right] = \left[\frac{d_c}{d_{eq} \left[\bar{\beta}(t)\right]} \right]^q = \frac{\bar{\beta}(t)\left[(1/d)^{q-s} - 1\right] + 1}{\left[\bar{\beta}(t)(d-1) + 1\right]^s} \quad (12)$$

2.3 Complete 0-D two-reach model

Rewriting the system (4) with the slopes $\bar{I}_U(t)$ and $\bar{I}_D(t)$ instead of the elevations $\bar{H}_U(t)$ and $\bar{H}_D(t)$ and using the Eqs. (10) and (11):

$$\begin{cases}
\frac{d\bar{I}_U}{dt} = \frac{2}{BL_U^2} \left[G(t) - P_U(t) - \frac{2L_U}{L_D} (P_U(t) - P_D(t)) \right] \\
\frac{d\bar{\beta}_U}{dt} = \frac{1}{BL_U \delta} \left[(\alpha_G(t) - \bar{\beta}_U(t)) G(t) - (\alpha_U(t) - \beta_U(t)) P_U(t) \right] \\
P_U(t) = M_U(t) Q(t)^m \\
M_U(t) = Cost \bar{I}_U(t) c_1 [\bar{\beta}_U(t)] \\
\frac{d\bar{I}_D}{dt} = \frac{2}{BL_D^2} [P_U(t) - P_D(t)] \\
\frac{d\bar{\beta}_D}{dt} = \frac{1}{BL_D \delta} \left[(\alpha_U(t) - \bar{\beta}_D(t)) P_U(t) - (\alpha_D(t) - \beta_D(t)) P_D(t) \right] \\
P_D(t) = M_D(t) Q(t)^m \\
M_D(t) = Cost \bar{I}_D(t) c_1 [\bar{\beta}_D(t)]
\end{cases} \quad (13)$$

Expressing the sediment discharge input from the watershed at the upstream end $P_U(x=0,t)$ as $G(t)$, the initial conditions of (13) are $G(t)$ and its composition $\alpha_G(t)$ at the upstream end, the elevation of the downstream end $\bar{H}_D(t)$ and the input of the liquid discharge $Q(t)^m$. If these conditions remain constant, at long time $t \rightarrow \infty$ the equilibrium can be reached: the sediment flux is spatially constant, and input and output become equal, i.e. $G(t) = P_U(t) = P_D(t)$ and $\alpha_G(t) = \alpha_U(t) = \alpha_D(t)$.

In their work, Di Silvio and Nones (2014) defined “filling volume” the relief volume that sediments can fill during a characteristic time of rivers named “filling time”. In (13), $\bar{B}L_U^2/2$ indicates the filling volume of the upstream reach $V_{0,U}$ divided by the slope $\bar{I}_U(t)$, and $\bar{B}L_D^2/2$ is the filling volume of the downstream reach $V_{0,D}$ divided by the slope $\bar{I}_D(t)$. In the same manner, the terms $L_U \delta \bar{B} = V_{m,U}$ and $L_D \delta \bar{B} = V_{m,D}$ are the filling volumes of the active layers of the upstream and downstream reach, respectively.

2.4 Non-dimensional formulation of the model

The problem is analysed introducing the dimensionless parameters reported in Table 1, defined as relative deviations from the equilibrium.

At long-term, the equilibrium values of sediment discharges $G(t \rightarrow \infty)$, $P_U(t \rightarrow \infty)$ and $P_D(t \rightarrow \infty)$ coincide, as well as the sediment parameters $\alpha_G(t \rightarrow \infty) = \alpha_U(t \rightarrow \infty) = \alpha_D(t \rightarrow \infty)$ and $\bar{\beta}_U(t \rightarrow \infty) = \bar{\beta}_D(t \rightarrow \infty)$. Marking such values as G_∞ , α_∞ and β_∞ , (13) can be rewritten in a dimensionless form.

$$\left\{ \begin{array}{l}
\frac{di_U}{dt} = \frac{G_\infty}{V_{0,U}} \left[g(t) - p_U(t) - \frac{2l_U}{l_D} (p_U(t) - p_D(t)) \right] \\
\frac{d\beta_U}{dt} = \frac{G_\infty}{V_{mix,U}} [(\alpha_G(t) - \beta_U(t))(g(t) + 1) - (\alpha_U(t) - \beta_U(t))(p_U(t) + 1)] \\
p_U(t) + 1 = [m_{orph,U}(t) + 1] [q(t)^m + 1] \\
m_{orph,U}(t) + 1 = [i_U(t) + 1]^n \frac{c_1(\beta_U(t))}{c_2(\beta_\infty)} \\
\frac{di_D}{dt} = \frac{G_\infty}{V_{0,D}} [p_U(t) - p_D(t)] \\
\frac{d\beta_D}{dt} = \frac{G_\infty}{V_{mix,D}} [(\alpha_U(t) - \beta_D(t))(p_U(t) + 1) - (\alpha_D(t) - \beta_D(t))(p_D(t) + 1)] \\
p_D(t) + 1 = [m_{orph,D}(t) + 1] [q(t)^m + 1] \\
m_{orph,D}(t) + 1 = [i_D(t) + 1]^n \frac{c_1(\beta_D(t))}{c_2(\beta_\infty)}
\end{array} \right. \quad (14)$$

Four characteristic times are recognizable: i) $V_{0,U}/G_\infty=T_{0,U}$ and $V_{0,D}/G_\infty=T_{0,D}$ indicate the filling times of the upstream and downstream reaches, respectively; ii) $\beta_\infty V_{mix,U}/G_\infty=T_{mix,U}$ and $\beta_\infty V_{mix,D}/G_\infty=T_{mix,D}$ are the filling times of the upstream and downstream active layers, respectively. The volume of the entire relief $V_{0,U}+V_{0,D}$ is greater than the volume of the total active layer $V_{mix,U}+V_{mix,D}$, while the evolution of the bed composition results faster than the evolution of the reach slope.

For the sake of simplicity, the water discharge $Q(t)$ is assumed constant during the river evolution, meaning that no significant natural or anthropogenic changes are considered in addition to the boundary conditions (i.e., the dimensionless parameter $q(t)^m$ is negligible). Under these assumptions, one finds $m_{orph,U}(t)=p_U(t)$ and $m_{orph,D}(t)=p_D(t)$, namely the non-dimensional perturbations of the morphodynamic parameter are equal to the non-dimensional perturbations of the sediment transport. Substituting these terms in (14) and deriving it over time to express the river morphodynamics evolution directly through the evolution of the perturbation of the parameter m_{orph} , one obtains:

$$\left\{ \begin{array}{l}
\frac{dm_{orph,U}}{dt} = [m_{orph,U}(t) + 1] \left[\frac{n}{i_U(t) + 1} \frac{di_U}{dt} + \frac{1}{c_1(\beta_U(t))} \frac{d(c_1(\beta_U(t)))}{d\beta_U} \frac{d\beta_U}{dt} \right] \\
\frac{dm_{orph,D}}{dt} = [m_{orph,D}(t) + 1] \left[\frac{n}{i_D(t) + 1} \frac{di_D}{dt} + \frac{1}{c_1(\beta_D(t))} \frac{d(c_1(\beta_D(t)))}{d\beta_D} \frac{d\beta_D}{dt} \right]
\end{array} \right. \quad (15)$$

The resulting model is implicit, non-linear and not analytically solvable. To find a simplified solution, one should linearize it assuming $m=n=2$ (i.e., uniform flow computed by the Chézy formula) and imposing that there are only little perturbations of the equilibrium conditions.

$$\left\{ \begin{array}{l} \frac{\overline{I_U(t)}^n}{I_\infty^n} = [1 + i_U(t)]^n \approx 1 + ni_U(t) = \left[1 + n \left(\frac{L_U + L_D}{L_U} h_U(t) - \frac{L_D}{L_U} h_D(t) \right) \right] \\ \frac{\overline{I_D(t)}^n}{I_\infty^n} = [1 + i_D(t)]^n \approx 1 + ni_D(t) = 1 + nh_D(t) \\ c_1 \beta_U(t) \approx c_1 \beta_\infty \left[1 + \beta_\infty \frac{1}{c_1 \beta_\infty} \frac{dc_1 \beta_U(t)}{d\beta_U} \Big|_{\beta_U(t)=\beta_\infty} \beta_U(t) \right] \\ c_1 \beta_D(t) \approx c_1 \beta_\infty \left[1 + \beta_\infty \frac{1}{c_1 \beta_\infty} \frac{dc_1 \beta_D(t)}{d\beta_D} \Big|_{\beta_D(t)=\beta_\infty} \beta_D(t) \right] \end{array} \right. \quad (16)$$

Substituting these equations in the definition of the perturbation of the morphodynamic parameter m_{orph} , an expression valid for both reaches is obtained:

$$m_{orph}(t) + 1 = [1 + n \cdot i(t)] [1 + \beta_\infty c_3(\beta_\infty) \beta(t)] \quad (17)$$

$$\text{where } c_3(\beta_\infty) = \frac{1}{c_1(\beta_\infty)} \frac{d(c_1(\beta(t)))}{d\beta} \Big|_{\beta(t)=\beta_\infty}.$$

However, the non-linearity remains in the mixed product $[i(t)b(t)]$. Unluckily, this non-explicit term is inside the formulation of $i(t)c_3[b(t)]$ and, therefore, it is not possible to reduce it by writing $i(t)b(t) \approx i_\infty b_\infty + i'(t)b_\infty + i_\infty b(t)$. To overcome the problem, a predictor-corrector scheme is applied, using an explicit Euler prediction scheme to compute the variables at the time $(t+\Delta t)$, cyclically corrected with a Crank-Nicholson algorithm until convergence.

3. Cases under study

3.1 Perturbation of the initial conditions

Knowing the time-averages external forcing terms $\overline{Q^m}$, \overline{G} and $\overline{\alpha_G}$, the equilibrium values of morphodynamic parameter, bottom composition and slope are:

$$\begin{cases} M_{\infty} = \frac{\overline{G}}{Q^m} \\ \beta_{\infty} = \frac{\overline{\alpha_G}}{(1/d)^{q-s} (1 - \overline{\alpha_G}) + \overline{\alpha_G}} \\ I_{\infty} = \left[\frac{M_{\infty}}{Cost} c_1(\beta_{\infty}) \right]^{1/n} \end{cases} \quad (18)$$

Aiming to compare the present model with the one proposed by Di Silvio and Nones (2014), a similar approach has been applied, investigating two types of initial conditions variations: stepwise and sinusoidal.

Recalling their work, stepwise perturbations are often connected to anthropogenic actions, while sinusoidal input variations are typically associated to the meteorological cycle (short period) or to geological and climate variations (long period), as pointed out by Blum and Törnqvist (2000). For the sake of simplicity, stepwise and sinusoidal variations are considered here only as perturbations in initial conditions, and do not alter the river evolution during the simulation (i.e., no sequences of sinusoidal/stepwise perturbations are considered).

3.1.1 Stepwise perturbation

From the equilibrium conditions, a stepwise perturbation of the solid input $G(t)$ at the upstream end is imposed.

$$\begin{cases} g(t) = 0 & \text{for } t = 0 \\ g(t) = g_0 & \text{for } t > 0 \end{cases} \quad (19)$$

The dimensionless value g_0 corresponds to a constant perturbation that leads the system to a new equilibrium, controlled by the sediment input $G_I = G(t > 0)$, different from the initial condition G_0 :

$$g_0 = \frac{G_1 - G_0}{G_0} \quad (20)$$

3.1.2 Sinusoidal perturbation

A sinusoidal perturbation of the sediment input has the form:

$$\begin{cases} g(t) = 0 & \text{for } t = 0 \\ g(t) = g_0 \sin(\omega t) & \text{for } t > 0 \end{cases} \quad (21)$$

where g_0 is the amplitude of the periodical input $g(t)$ and $\omega=2\pi/T_w$ is the angular frequency linked to the forcing period T_w of $g(t)$. In this manner, the quasi-equilibrium condition reached after a transitory stage results periodical.

3.2 Input data

To show the model potential, the effects of the changing initial conditions are evaluated considering quantities typical of alluvial rivers in temperate climates. In the simulations (Eqs. 5 and 6) it is assumed $m=2$, $s=0.5$ and $\alpha_{EH}=10^{-3}$, while the grain-size composition is characterized by $d_f=0.5$ mm and $d_c=12.5$ mm ($d=0.04$) and the constant river width B is assumed equal to 50 m (Franzoia, 2014).

4. Results and discussion

The outcomes of the two-reach model are compared with the results obtained by Di Silvio and Nones (2014), whom have schematized the river as a single reach with a uniform slope from the basin barycenter to the downstream end, having a fixed elevation and a constant width. Moreover, their model assumed a constant grain-size of the bed sediments, and the only time-dependent variable was the slope.

Assuming $\bar{I}_U=\bar{I}_D$ (or $L_D=0$) and $P_U(t)=P_D(t)$, one obtains $P_U(t)=Cost_I\bar{I}_U(t)^n=Cost_I\bar{I}_D(t)^n=P_D(t)$, and the dimensionless terms $i_U(t)$ and $i_D(t)$ coincide, having also $h_U(t)=h_D(t)$. Imposing $m=n=2$, Di Silvio and Nones (2014) have linearized the problem through $(1+i_U(t))^n=(1+i_U(t))^2\approx(1+2i_U(t))=(1+2h_U(t))$, obtaining $p_U(t)=2h_U(t)$ and an ordinary differential equation that described the morphological evolution of the river reach:

$$\frac{dh_U}{dt} = \frac{1}{T_{0,U}} [g(t) - 2h_U(t)] \quad (22)$$

Using the approach described here, the characteristic filling time $T_{0,U}$ for the upstream reach is a trapezoidal volume based on the position of the gauging stations (Fig. 1).

$$T_{0,U} = \frac{2G_0}{H_0 L_U B [2 - L_U / (L_U + L_D)]} \quad (23)$$

The filling volume computed by Di Silvio and Nones (2014) results greater than the filling volume of the model with two reaches, but the time required to attain the equilibrium is smaller.

4.1 Perturbations of the sediment input amount

Many 1-D hydro-morphodynamic models found out that perturbations in the grain-size distribution propagate at a faster pace than adjustments in the bed elevation, possibly due to "sorting" (Stecca et al., 2014) or "mixing" (Ribberink, 1987) waves, which, generally, have a higher celerity than the bed waves.

The reaction of a schematic river initially in equilibrium in response to stepwise or sinusoidal perturbations of the initial sediment input $G(t)$ is here analyzed, aiming to reproduce these results with a simpler model.

4.1.1 Stepwise perturbation

Starting from equilibrium conditions, a stepwise perturbation $g(t)$ is imposed, which corresponds to a constant perturbation that leads the system to a new equilibrium controlled by the sediment input $G_1 = G(t > 0) \neq G_0$.

The results obtained for a river having $L_U = 0.2L_D$ and subjected to a perturbation $g_0 = 0.2$, reported in Fig. 2, show that, after a stepwise increase of the sediment input, firstly a rapid fining of the bottom composition $\beta(t)$ is observed, leading to a rapid increase of the morphodynamic parameter $M(t)$. Then a slower phase takes place, during which the bottom slope $I(t)$ increases towards the equilibrium value I_∞ , and the bottom composition becomes finer, equal to the equilibrium value β_∞ . In these conditions, the equilibrium morphodynamic parameter M_∞ depends only on the slope variations.

The outcomes are function of the upstream/downstream reach lengths ratio L_U/L_D . Increasing the length of the upstream part, its evolution celerity decreases and the trend of the two reaches tends to coincide. In Figure 3a are reported the slope variations and the evolution of the morphodynamic parameters for a schematic two-reach river having a negligible length of the downstream reach ($L_U/L_D = 5$). The solutions for this reach are almost equal to the solutions for the upstream part (i.e., with only one reach, Figure 3b).

With the linearized solution proposed by Di Silvio and Nones (2014) and imposing the initial condition $h_U(t=0) = 0$, the integration of (22) yields to:

$$h_U(t) = \frac{g_0}{2} \left(1 - e^{-2t/T_{0,U}} \right) \quad (24)$$

Assuming $h_U(t) = 2p_U(t)$:

$$p_U(t) = g_0 \left(1 - e^{-2t/T_{0,U}} \right) \quad (25)$$

Figure 3b reports the temporal evolution of a single-reach river having a constant grain-size composition, subjected to a stepwise perturbation $g_0=0.2$, discerning between different slope ratios I_U/I_∞ .

The evolution of the approach proposed here, having the exact solution numerically computed and a variable bottom composition, is slower than the one obtained with the linearized solution proposed by Di Silvio and Nones (2014), whom considered unisize sediments. This fact gives reason to the need of considering mixed grain-sizes during the evaluation of the river adaptation time (Church & Ferguson, 2015).

The comparison between the evolution of a bed having a sorted grain-size ($d=0.04$) and one with a uniform composition ($d=1$) reported in Figure 4 highlights the behaviour described above: a well-sorted bed evolves faster with respect to poorly sorted rivers, reaching the equilibrium in a temporal horizon in the order of some decades rather than centuries.

4.1.2 Sinusoidal perturbation

Assuming the perturbation of the sediment input $g(t)$ sinusoidally variable in time, the equilibrium conditions are defined averaging the values over a longer time, namely the forcing period T_w . As expected, in this case the results are related to the length ratio L_U/L_D : with a relevant length of the downstream reach the solution for the two reaches sensibly differ from the solution computed with a single reach. Increasing the period T_w one finds a limit for which the perturbation is more similar to a stepwise alteration, because the time required to reach the new equilibrium is lower than $T_w/4$ (Franzoia, 2014).

4.2 Perturbation of the sediment input composition

A stepwise perturbation $\alpha_{G,0}$ of the composition of the sediment input $\alpha_G(t)$ is:

$$\begin{cases} \alpha_G(t) = 0 & \text{for } t = 0 \\ \alpha_G(t) = \alpha_{G,0} = \frac{\alpha_G(t > 0) - \alpha_G(t < 0)}{\alpha_G(t < 0)} & \text{for } t > 0 \end{cases} \quad (26)$$

where $\alpha_G(t > 0)$ is the perturbation of the input in terms of sediment composition.

Confirming the outcomes of laboratory experiments (Ribberink, 1987) and numerical 1-D fully unsteady models (Blom, 2008; Stecca et al., 2016), the present results highlight that the perturbation of the sediment input composition can substantially modify the river slope, especially at the long-term. Figure 5 shows the evolution of a river when the sediment input becomes finer, with a stepwise perturbation of the solid input composition $\alpha_{G,0}=0.05$. Though the equilibrium morphodynamic coefficient $M_\infty=G_\infty/Q^m$ remains the same, the equilibrium bed composition is finer, hence the equilibrium slope decreases. There a rapid fining of the bed initiates, followed by a very long period required to attain a new equilibrium, during which the slope changes very slowly, while the morphodynamic parameter increases responding to the fining, and then slowly decreases till the equilibrium.

4.3 Perturbation of the liquid discharge input

The initial hypothesis was that no substantial variations of the liquid flow are considered, aiming to simplify the equations, finding that the perturbation on the sediment discharge corresponds to the perturbation of the morphodynamic parameter, i.e. $p(t)=m_{orph}(t)$.

On the contrary, considering a perturbation of the liquid discharge $q(t)^m$ means that there is a variation of the flow duration curve, typical of real-world watercourses. Assuming the validity of the LUF hypothesis, the only parameter that is supposed to change in the equation of the morphological evolution is the thickness of the active layer δ . This value is taken as a fraction of the mean water depth in dune-dominated contexts, where dunes represent the feature that operate the vertical mixing, and thus naturally the active layer scales with dune height, which scales with water depth. Conversely, it is taken as a multiple of the d_{90} in plane-bed cases.

Considering only the influence of the liquid phase on the equilibrium formula, the perturbation of the sediment transport $p(t)$ is:

$$p(t) = \left[m_{orphU}(t) + 1 \right] \left[q(t)^m + 1 \right] - 1 \quad (27)$$

In Figure 6 a comparison of the evolution of the morphodynamic parameter $M(t)$ with different forcing periods T_w is reported, showing the evolution of the ratio $M(t)/M_\infty$ for limited temporal horizons.

Under a physical point of view, a series of perturbations of the liquid flow duration curve characterized by a sinusoidal behaviour with different forcing periods T_w can represent the natural long-term variations of the climatic conditions acting in a watershed.

4.4 Long-term evolution of rivers

Numerical simulations show that, for any initial condition, the variables swing to reach the same results, namely the two reaches slowly evolves towards the equilibrium. In these conditions the downstream reach has a smaller slope and a finer bed composition than the upstream part, maintaining the features of a concave profile characterized by a downstream fining (e.g., Ferrer-Boix et al., 2016; Gomez et al., 2001; Leopold & Maddock, 1953; Rice & Church, 2001; Richter, 1939; Shulits, 1941; Sinha & Parker, 1996; Snow & Slingerland, 1987).

The results reported in Figure 7 show that, starting from an initial condition, even if convex and with a uniform bed composition, the river morphology evolves towards a concave profile with downstream fining before reaching the equilibrium, considering an upstream reach either shorter or longer than the downstream one.

In Figure 8 the temporal evolutions of bottom composition $\beta(t)$, slope $I(t)$ and morphodynamic parameter $M(t)$ are shown for an upstream reach shorter than the downstream one. In particular, the evolution of the grain-size composition $\beta(t)$ is highlighted in Figure 9: starting from a bed composition equal to the equilibrium, the sediments rapidly become finer and then a slow evolution towards a coarse grain-size composition starts, with respect to the downstream fining characteristics.

5. Conclusions

Aiming to replicate previous results obtained with more complex approaches, the 0-D model developed here is physically-based on typical hydro-morphological equations, even if described in a very simplified manner. Theoretically, the parameters used by physically-based models are measurable, but, in practice, this kind of codes needs to be calibrated and verified against observed data, because of the large number of parameters involved and the heterogeneity of their values. A typical dataset is formed by a continuous record of water flowing through a given cross section and some basin-scale averaged geometrical (river slope, width, length) and sedimentological (grain-size) information. In this regard, continuous records of sediment transport and water flow are necessary to calibrate and validate such models.

The proposed mathematical system results implicit and non-linear and, therefore, it is not possible to find an analytical solution. For this reason, a numerical evaluation based on a

predictor-corrector scheme is applied, showing the potential of the approach despite of the several simplifications involved. Solving 0-D models is much simpler and faster than solving a complete 1-D hydro-morphodynamic model, with a reduced loss of details at the large spatial and temporal scale.

With respect to previous conceptualizations (Di Silvio & Nones, 2014), assuming a non-uniform grain-size composition, crucial in the erosion/deposition phenomena, and splitting the river in two connected LUF reaches representing the highland and the lowland parts, the morphological evolution of the schematic river results realistically slow. Moreover, the present model shows the typical processes of alluvial rivers, characterized by a downstream fining and an evolution towards a concave longitudinal profile, starting from altered initial conditions in terms of sediment transport and/or water flow. On the one hand, the outcomes are in accordance with literature evidences (e.g., Church & Ferguson, 2015; Costigan et al., 2014; Cui et al., 1996; Frings, 2008; Gasparini et al., 2004; Paola & Seal, 1995; Sinha & Parker, 1996). On the other hand, the 0-D modelling of the long-term evolution of watercourses requires very crude schematizations, aiming to simulate the behaviour of alluvial rivers under specific constraints with a reduced computational effort. Obviously, this condition is very far from the situation observed in nature because, at the long-time scale, initial and boundary conditions are not constant, but a lot of processes can take place, such as variations in the natural hydrologic regime possibly driven by climate change, human interventions like dam building, dredging operations or deforestation projects. Indeed, this schematization is more like a laboratory flume, feed with a constant input of sediments. Given that mountains are not an infinite source of sediments (Park & Jain, 1987), all these alterations can affect the river evolution. It is worth to mention that, even is mountains cannot be considered as infinite sources of sediment, in some cases the tectonic uplift is likely able to renew the sources given by slope, possibly at a pace higher than the transport capability of the watercourses.

As previously observed, the evolution of the river morphology studied by the present two-reach model with non-uniform grain-size results slower than the one analyzed by Di Silvio and Nones (2014). In fact, their model neglects the variability of the bed composition, and did not consider the fundamental role played by the bottom composition, as recognizable from the analyses of the river reaction to the perturbation of the initial conditions and of the very long-term evolution. Even if the proposed model does not operate directly on the grain-size parameters, the bottom composition reacts very rapidly to any perturbation, changing the behaviour of the system itself

via the morphodynamic parameter. After an initial state, the evolution slows down, following the evolving time of the slopes, i.e. reaching the equilibrium in about four times the characteristic filling time of the longer reach. In this sense, the present model is a significant improvement of the previous approach (Di Silvio & Nones, 2014), especially for its capability to represent the observed behaviour of alluvial watercourses with a reduced computational effort.

Additional research is necessary to: i) evaluate the reliability of the model in simulating the effects of initial conditions that subsequently vary during the watershed evolution, instead of single variations as proposed here; ii) discuss the importance of a changing width in computing the long-term evolution of alluvial rivers; iii) define the relative importance of the adopted river parameters and the simplifications used, possibly applying the model to real case studies.

Acknowledgements

The Authors warmly thank Prof. Giampaolo Di Silvio, who has contributed to the quality of the research with very constructive hints and discussions. A kind thanks goes to the reviewers, which spent a lot of time in revising the manuscript, adding very interesting comments and improving the overall quality of the research.

References

- Armanini, A., & Di Silvio, G. (1988). A one-dimensional model for the transport of a sediment mixture in non-equilibrium conditions. *Journal of Hydraulic Research*, 26, 275–292.
- Asselman, N.E.M. (2000). Fitting and interpretation of sediment rating curves. *Journal of Hydrology*, 234, 228–248.
- Bai, Y., & Wang, Z. (2014). Theory and application of nonlinear river dynamics. *International Journal of Sediment Research*, 29, 285–303.
- Ballio, F., Nikora, V., & Coleman, S.E. (2014). On the definition of solid discharge in hydro-environment research and applications. *Journal of Hydraulic Research*, 52, 173–184.

- Basile, P.A. (1994). *Modellazione dei meccanismi di intercettazione e rilascio di sedimenti da parte delle briglie permeabili*. PhD. Thesis, IMAGE Department, University of Padova, Italy. (In Italian)
- Blom, A. (2008). Different approaches to handling vertical and streamwise sorting in modeling river morphodynamics. *Water Resources Research*, 44(W03415).
- Blum, M.D., & Törnqvist, T.E. (2000) Fluvial responses to climate and sea-level change: a review and look forward. *Sedimentology*, 47, 2-48.
- Church, M., & Ferguson, R.I. (2015). Morphodynamics: Rivers beyond steady state. *Water Resources Research*, 51, 1883-1897.
- Colby, B.R. (1956). *Relationship of sediment discharge to streamflow*. US Dept. of the Interior, Geological Survey, Water Resources Division, No. 56-27.
- Costigan, K.H., Daniels, M.D., Perkin, J.S., & Gido, K.B. (2014). Longitudinal variability in hydraulic geometry and substrate characteristics of a Great Plains sand-bed river. *Geomorphology*, 210, 48-58.
- Cui, Y., Paola, C., & Parker, G. (1996). Numerical simulation of aggradation and downstream fining. *Journal of Hydraulic Research*, 34, 185-204.
- De Vriend, H., Zyserman, J., Nicholson, J., Roelvink, J., Pechon, P., & Southgate, H. (1993). Medium-term 2dh coastal area modelling. *Journal of Coastal Engineering*, 21, 193–224.
- Di Silvio, G., & Nones, M. (2014). Morphodynamic reaction of a schematic river to sediment input changes: Analytical approaches. *Geomorphology*, 215, 74–82.
- Engelund, F., & Hansen, E. (1967). *A monograph on sediment transport in alluvial streams*. TEKNISKFORLAG. Copenhagen, Denmark.
- Exner, F.M. (1920). *Zur Physik der Dunen*. Sitzber Akad. Wiss Wien, Part IIa, Bd. 129. (In German)
- Fasolato, G., Ronco, P., & Di Silvio, G. (2009) How fast and how far do variable boundary conditions affect river morphodynamics?. *Journal of Hydraulic Research*, 47, 329–339.

- Fasolato, G., Ronco, P., Langendoen, E.J., & Di Silvio, G. (2011). Validity of Uniform Flow Hypothesis in One-Dimensional Morphodynamics Models. *Journal of Hydraulic Engineering-ASCE*, *137*, 183–195.
- Ferrer-Boix, C., Chartrand, S.M., Hassan, M.A., Martin-Vide, J.P., & Parker, G. (2016). On how spatial variations of channel width influence river profile curvature. *Geophysical Research Letter*, *43*, 6313-6323.
- Franzoia, M. (2014). *Sediment yield in rivers at different time-scales*. PhD Thesis. DICEA Department University of Padova, Italy. Available at <http://paduaresearch.cab.unipd.it/6382/>
- Frings, R.M. (2008). Downstream fining in large sand-bed rivers. *Earth-Science Reviews*, *87*, 39-60.
- Gasparini, N.M., Tucker, G.E., & Bras, R.L. (2004). Network-scale dynamics of grain-size sorting: implications for downstream fining, stream-profile concavity, and drainage basin morphology. *Earth Surface Processes and Landforms*, *29*, 401-421.
- Gomez, B., Rosser, B.J., Peacock, D.H., Hicks, D.M., & Palmer, J.A. (2001). Downstream fining in a rapidly aggrading gravel bed river. *Water Resources Research*, *37*, 1813-1823.
- Gourbesville, P. (2009). Data and hydroinformatics: new possibilities and challenges. *Journal of Hydroinformatics*, *11*, 330-343.
- Guinot, V., & Gourbesville, P. (2003). Calibration of physically based models: back to basics? *Journal of Hydroinformatics*, *5*, 233-244.
- Hirano, M. (1971). River bed degradation with armouring. *Proceedings of the Japan Society of Civil Engineers*, *195*. (In Japanese)
- Hobley, D.E., Adams, J.M., Nudurupati, S.S., Hutton, E.W., Gasparini, N.M., Istanbuluoglu, E. & Tucker, G.E. (2017). Creative computing with Landlab: an open-source toolkit for building, coupling, and exploring two-dimensional numerical models of Earth-surface dynamics. *Earth Surface Dynamics*, *5*, 21-46.
- Horowitz, A.J. (2003). An evaluation of sediment rating curves for estimating suspended sediment concentrations for subsequent flux calculations. *Hydrological Processes*, *17*, 3387–3409.

- Juez C., Murillo J., & García-Navarro P. (2013). Numerical assessment of bed-load discharge formulations for transient flow in 1D and 2D situations. *Journal of Hydroinformatics*, 15, 1234-1257.
- Leopold, L.B., & Maddock, T. (1953). The hydraulic geometry of stream channel and some physiographic implications. *Prof. Pap.*, 252, U.S. Geol. Surv., Washington D. C.
- Lyn, D.A. (1987). Unsteady sediment transport modeling. *Journal of Hydraulic Engineering, ASCE*, 113, 1-15.
- Lyn, D.A., & Altinakar, M. (2002). St. Venant Exner equations for near-critical and transcritical flows. *Journal of Hydraulic Engineering, ASCE*, 128, 579-587.
- Nones, M. (2012). *Aspects of riverine hydro-morpho-biodynamics at watershed scale*. PhD thesis, IMAGE Department, University of Padova, Italy. Available at http://paduaresearch.cab.unipd.it/4468/3/PhD_Thesis.pdf
- Nones, M. & Di Silvio, G. (2016). Modeling of river width variations based on hydrological, morphological and biological dynamics. *Journal of Hydraulic Engineering-ASCE*, 142, 04016012.
- Paola, C. & Seal, R. (1995). Grain size patchiness as a cause of selective deposition and downstream fining. *Water Resources Research*, 31, 1395–1407.
- Park, I., & Jain, S.C. (1987) Numerical simulation of degradation of alluvial channel beds. *Journal of Hydraulic Engineering*, 113, 845–859.
- Ribberink, J.S. (1987). *Mathematical modelling of one-dimensional morphological changes in rivers with non-uniform sediment*. PhD thesis, Faculty of Civil Engineering and Geosciences, Delft University of Technology, Delft, The Netherlands. Available at <http://repository.tudelft.nl/view/ir/uuid%3Abdfc1519-a71d-4752-83f7-3ebf1bb890e9/>.
- Rice, S.P., & Church, M. (2001). Longitudinal profiles in simple alluvial systems. *Water Resources Research*, 37, 417–426.
- Richter, J.P. (1939). *The Literary Works of Leonardo da Vinci*. Vol. 2, 438 pp., Oxford Univ. Press, New York.
- Shulits, S. (1941). Rational equation of river-bed profile. *Eos Trans. AGU*, 22, 622–630.

- Sinha, S., & Parker, G. (1996). Causes of concavity in longitudinal profiles of rivers. *Water Resources Research*, 32, 1417–1428.
- Snow, R.S., & Slingerland, R.L. (1987). Mathematical modeling of graded river profiles. *The Journal of Geology*, 95, 15–33.
- Stecca, G., Siviglia, A., & Blom, A. (2014). Mathematical analysis of the Saint-Venant-Hirano model for mixed-sediment morphodynamics. *Water Resources Research*, 50, 7563-7589.
- Stecca, G., Siviglia, A., & Blom, A. (2016). An accurate numerical solution to the Saint-Venant-Hirano model for mixed-sediment morphodynamics in rivers. *Advances in Water Resources*, 93, 39-61.
- Tealdi, S., Camporeale, C., & Ridolfi, L. (2011). Long-term morphological river response to hydrological changes. *Advances in Water Resources*, 34, 1643–1655.
- Vidal, J.P., Moisan, S., Faure, J.B., & Dartus, D. (2005). Towards a reasoned 1D river model calibration. *Journal of Hydroinformatics*, 7, 91-104.
- Walling, D.E. (1974). Suspended sediment and solute yields from a small catchment prior to urbanization. In: Gregory, K.J., Walling, D.E. (Eds.). *Fluvial processes in instrumented watersheds*, Institute of British geographers, Special publication, 6, 169–192.

Figure 1. Scheme of the zero-dimensional, two-reach model.

Figure 2. Evolution of a schematic river with $L_U=0.2 L_D$ and $d=0.04$, applying a stepwise perturbation of the sediment input $g_0=0.2$: a) ratio between the bottom composition $\beta(t)$ and its equilibrium value β_∞ ; b) ratio between the river slope $I(t)$ and its equilibrium value I_∞ ; c) ratio between the morphodynamic parameter $M(t)$ and its equilibrium value M_∞ .

Figure 3. Comparison of morphodynamic parameter and slope evolution: a) river modelled as two-reach and sorted grain-size, assuming $L_U/L_D=5$ and imposing a stepwise perturbation of the sediment input $g_0=0.2$; b) river modelled as single reach and with constant grain size, applying a stepwise perturbation $g_0=0.2$.

Figure 4. Evolution of a schematic river with $L_U=0.2 L_D$ and $d=1$, applying a stepwise perturbation of the sediment input $g_0=0.2$: a) ratio between the river slope $I(t)$ and its equilibrium value I_∞ ; b) ratio between the morphodynamic parameter $M(t)$ and its equilibrium value M_∞ .

Figure 5. Evolution of a schematic river with $L_U=0.2 L_D$ from an initial equilibrium state applying a stepwise perturbation $\alpha_{G,0}=0.05$: a) ratio between the bottom composition $\beta(t)$ and its equilibrium value β_∞ ; b) ratio between the river slope $I(t)$ and its equilibrium value I_∞ ; c) ratio between the morphodynamic parameter $M(t)$ and its equilibrium value M_∞ .

Figure 6. Temporal evolution of the morphodynamic parameter $M(t)$ with respect to its equilibrium value, applying a sinusoidal perturbation of the discharge input $q^m(t>0)=q^m_{G,0} \sin \omega t$ with $q^m_{G,0}=0.1$, $L_U=0.2L_D$ and for different periods T_w .

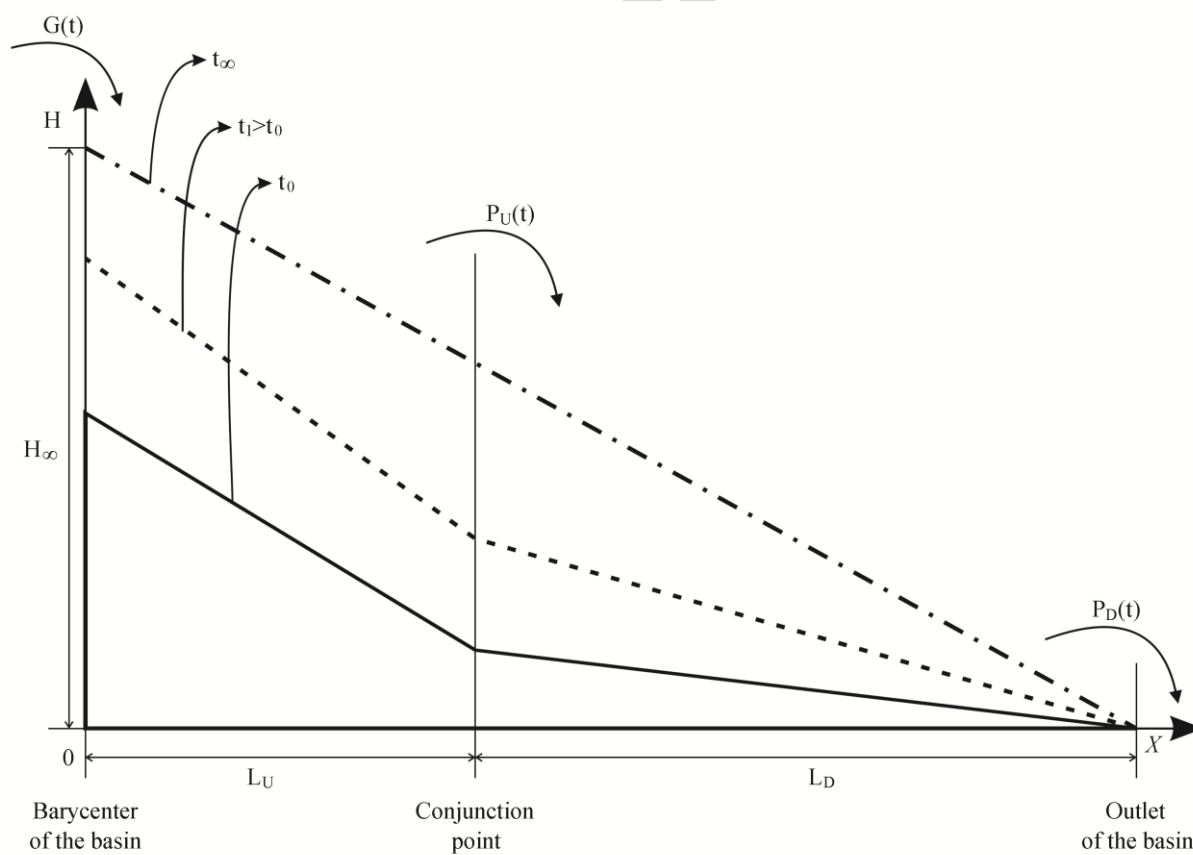
Figure 7. Very long-term evolution of the longitudinal profile of a schematic river, starting from a convex longitudinal profile: a) $L_U=0.2 L_D$; b) $L_U=5 L_D$.

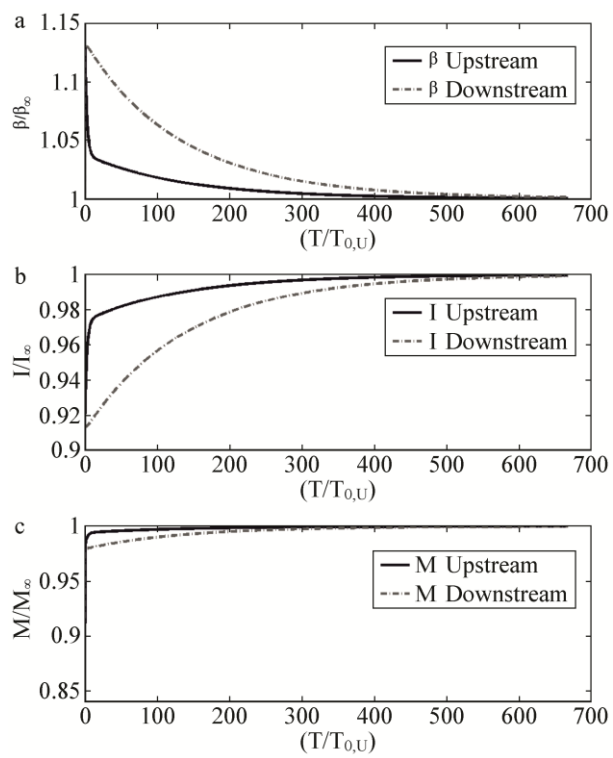
Figure 8. Evolution of a schematic river with $L_U=0.2 L_D$ and $d=0.04$, starting from a convex longitudinal profile and an equilibrium bottom composition: a) ratio between the bottom composition $\beta(t)$ and its equilibrium value β_∞ ; b) ratio between the river slope $I(t)$ and its equilibrium value I_∞ ; c) ratio between the morphodynamic parameter $M(t)$ and its equilibrium value M_∞ .

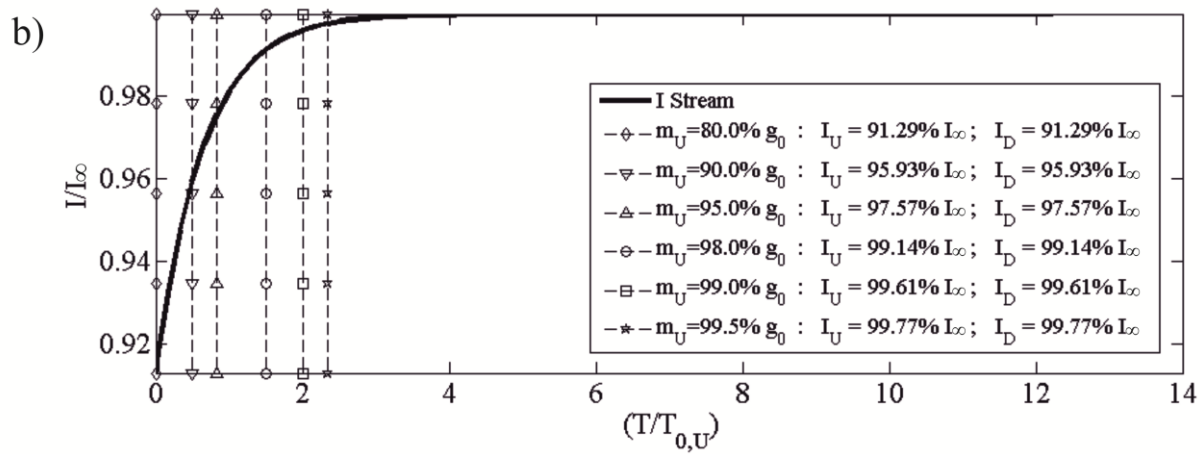
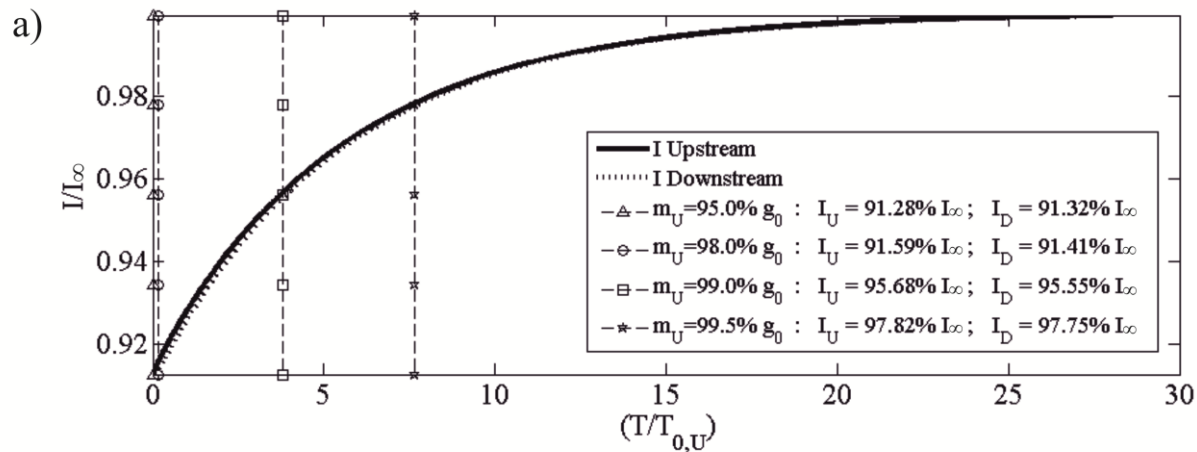
Figure 9. Zoom of the initial period reported in Figure 8a.

Table 1. List of dimensional and dimensionless parameters.

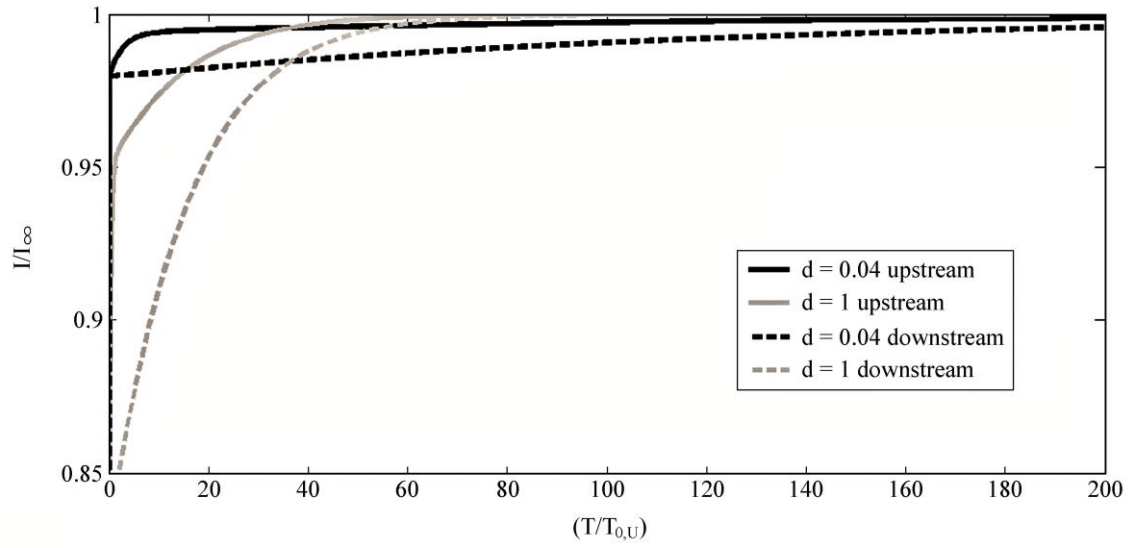
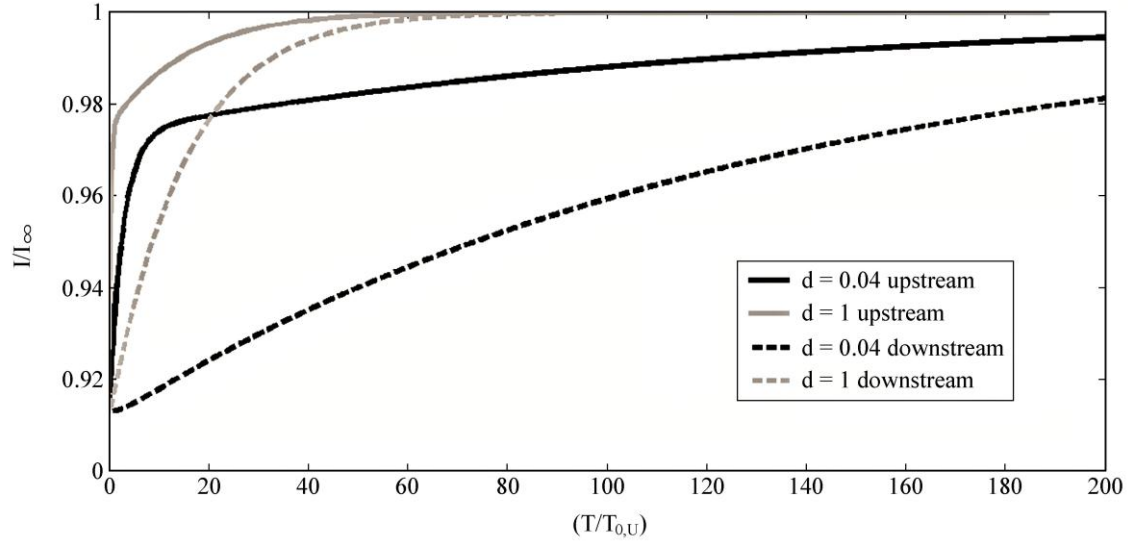
Dimensional parameters	Non-dimensional parameters
$\overline{H_U}, \overline{H_D}$	h_U, h_D
L_U, L_D	l_U, l_D
$\overline{I_U}, \overline{I_D}$	i_U, i_D
P_U, P_D	p_U, p_D
G	g
Q^m	q^m
M_U, M_D	$m_{\text{orph,U}}, m_{\text{orph,D}}$







Accepted



Accer

